FIR FILTER DESIGN USING HIGHLY NON-LINEAR LADF SIGMA-DELTA (Σ-Δ) MODULATOR ARCHITECTURE

Kabi Prakash Padhi, Tan Chin Tiong and Saman S. Abeysekera

School of Electrical and Electronic Engineering
Nanyang Technological University
Block S1, Nanyang Avenue, Singapore 639798.
Ph: +65 790 4515, Fax: +65 793 3318, E-mail: esabeysekera@ntu.edu.sg

ABSTRACT

In this paper we investigate the performance of multiplier free FIR filter design using an extremely non-linear Σ-Δ architecture. This architecture which is known as the Look Ahead Decision Feedback (LADF) circuit [1], has not been used in FIR filter design earlier. The circuit is highly non-linear because of the thresholding operation in the architecture. In this paper, we compare the LADF architecture with other conventional Σ-Δ architectures in the design of FIR filters. The noise characteristics of these architectures are discussed. It will be shown that the LADF architecture has relatively low noise power at low frequencies in comparison to other modulators. The design of optimum lowpass filters and comb filters for good noise reduction for LADF architecture is also addressed in the paper. Using a lowpass FIR filter design example, the appropriate filter design methodology is presented in the paper.

1. INTRODUCTION

Sigma-Delta (Σ-Δ) modulators have been widely used for both A/D and D/A conversion schemes. The basis of sigma-delta modulation schemes is the principle of oversampling the input. As sampling is done above the Nyquist rate, the noise power is uniformly distributed over the larger frequency range, thereby improving the resolution. The noise power beyond the signal bandwidth can be removed by using a lowpass filter. The output is then downsampled to the Nyquist rate.

For some time, Σ-Δ modulators have been proposed for other applications in signal processing, such as FIR and IIR filter design, AM/FM modulators, correlators, multipliers and synchronizers [2][3]. A major reason for the popularity of Σ-Δ architectures lie in their ability to trade bandwidth with quantization noise. These circuits lead to reduced inexpensive hardware and help in speeding up computations besides providing higher resolution in comparison to traditional analogue circuitry. Furthermore, as the Σ-Δ modulated signals are restricted to take values of {-1, 0, +1}, the Σ-Δ based signal processing architecture provides programmability and flexibility in the circuits.

Consider the FIR filter design via the use of Σ-Δ modulators. It is worth noting here some of the problems faced in the traditional FIR filter implementation. These are :

i) The resolution is limited by the resolution of the ADC.

ii) Multi-bit adders and multipliers are needed which use complex hardware. They also increase the overall cost of the device where high precision is required.

iii) Hardware once designed cannot be changed. Though DSPs are more flexible, they are more expensive.

Due to these problems, Σ-Δ modulation is a more affordable option of implementing FIR filters. The 1-bit output of these modulators removes the need for multi-bit multipliers and hence decreases the complexity and cost of the circuit. Besides this, resolution is improved due to over-sampling before modulation. Multipliers can be entirely eliminated from the circuit by using shift registers to process the 1-bit output of the modulator [4].

2. Σ-Δ MODULATOR ARCHITECTURES

Conventionally, the performance of the Σ-Δ modulators are improved by the use of multi-loop (identified here as DSM) or multi-stage (MASH) architectures [5][6]. Recently, another method of Σ-Δ modulation, known as Look Ahead Decision Feedback (LADF) technique, has been proposed by Stonick et. al. [1]. In this paper, we compare the use of above three Σ–Δ modulator architectures in the design of FIR filters. A brief description of the LADF architecture is also presented here.

2.1 3rd order LADF (LADF3) modulator:

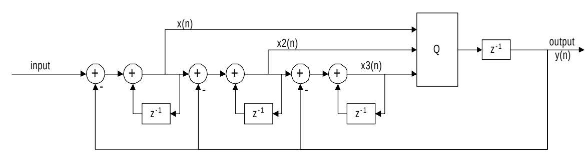

Figure 1: 3rd order LADF modulator

As the name suggests, the LADF architecture has two distinguishing features, namely – look-ahead and decision feedback. The modulator is designed on the concept - starting with the multi-loop structure, a one-bit output is chosen at each time-state, so that the set of integrator outputs at the next state are most stable. Thus, the architecture *looks-ahead* at the possible future states and *feeds-back* this information to the current output decision. For example, Figure 1 shows the architecture of a 3rd order LADF modulator. In Figure 1, *x(n), x2(n)* and *x3(n)* comprise the look-ahead section while the feedback section is the return path from *y(n)*. To determine the most stable set of states, the LADF algorithm chooses an output, which minimizes a cost function of the integrators at each time state. The quantizer adds the uncertainty or noise to the system.

Hence, it can be modeled by an error term. Under these conditions, the function *q(n)* of block *Q* in Figure 1 is obtained as follows :

$$q(n) = \mathrm{sgn}\{\frac{1}{6}|x3(n)+1|^3 - \frac{1}{6}|x3(n)-1|^3 + 2(x2(n)+x3(n)) - |x(n)+x2(n)+x3(n)-3| + |x(n)+x2(n)+x3(n)+3|\} \qquad Eq.1$$

where, the *sgn* (or *signum)* function is a 2-level quantizer with output levels {-1,+1}.

2.2 Spectral Characteristics of Quantization Noise:

It is possible to compare the various **Σ-Δ** modulator architectures by observing their quantization noise characteristics. A quantity that can be used in this comparison is the filtered quantization noise power resulting from an ideal lowpass filter of bandwidth f_c. The filtered quantization noise power - $P(f_c)$, for double loop modulator (DSM2), 3rd order multi-stage (MASH3) modulator and the 3rd order LADF modulator (LADF3) are approximately given by the following equations as discussed in [3].

$$DSM2: P(f_c) = \sin^2(\pi.f_c)/3$$
$$MASH3: P(f_c) = 8.\sin^4(\pi.f_c)/3$$
$$LADF3: P(f_c) = 800.\sin^4(\pi.f_c)/3 \qquad Eq.2$$

Figure 2 shows filtered quantization power $P(f_c)$ vs. filter bandwidth f_c, obtained using simulations. For the simulations 8192 samples were used and the Σ-Δ modulator input was selected as a dc signal. The slope of the plots in Figure 2 corroborates with the predicted values from equation 2.

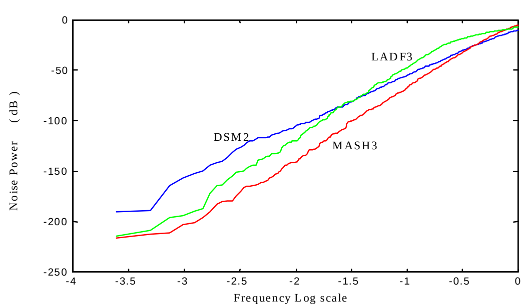

Figure 2: Filtered Quantization Noise Power vs. Bandwidth

Note that in Figure 2, the slope of the DSM2 curve is 50 while that of the LADF3 and MASH3 architectures is 70. The value at 0 frequency corresponds to the total noise power resulting from the modulator. It can also be seen that the MASH3 circuit performs better than the other architectures, while LADF3 is better than DSM2 in the low frequency. The intersection point of the curves gives the frequency at which the LADF3 noise worsens than the DSM2. The LADF3 circuits results in a *20dB* higher noise power in comparison to the MASH3 architecture.

2.3 Coefficient Histograms:

In order to consider the suitability of the above three Σ-Δ modulator architectures in multiplier free FIR filter design, it is necessary to observe the modulator output coefficient distributions. The following Table 1 shows the coefficient histograms for the DSM2, MASH3 and LADF3 modulators. Note that DSM2 and MASH3 modulators were implemented using 3-level quantizers {-1, 0 +1}. This is because it has been observed that 3-level quantizers result in smaller quantization noise power when compared to 2-level quantizers. However, LADF3 architecture was implemented using a 2-level quantizer as the LADF circuit was specifically designed to be used with a 2-level quantizer.

Coeffs.	-3	-2	-1	0	1	2	3
DSM2	-	-	21	49	30	-	-
MASH3	2	10	20	30	24	12	2
LADF3	-	-	45	-	55	-	-

Table 1: Output Coefficient Histograms (%)

The coefficient histograms in Table 1 show that both DSM2 and MASH3 generate substantial number of zero coefficients because of the 3 level quantizers. This decreases the circuit complexity in implementing FIR filters, as zero coefficients avoid multipliers. It can be seen that the LADF3 architecture needs more number of multiplications as it has a 2 level quantizer. It can also be observed that the number of 1's and -1's are approximately equally distributed in the case of the LADF3 and DSM2 modulators. However, the number of 0 coefficients in DSM2, amount to 50 % of the total number of filter coefficients. It should be noted that MASH3 structure might produce ±4 as an output because it has 3 quantizers and an additional outer loop.

3. DEMODULATORS

At the demodulator, the high frequency quantization noise produced by the Σ-Δ modulator is filtered out by a lowpass filter to recover the slowly varying input signal. Suitable demodulator lowpass filters such as Comb filters [8], Optimum FIR filters [5] and Laguerre IIR filters [10] have been proposed in the literature. Some of these filters which can be used in the design of Σ-Δ modulator based FIR filters are discussed in the following section.

3.1 Optimum FIR filters:

These are based on minimizing the quantization noise of Σ-Δ modulators under constraint equations. Let *L* denote the order of the modulator. It is taken to be 2 and 3 in the example discussed later. The filtered noise power ψ is then given by :

$$\psi = \int_0^1 |2.\sin(\pi f)|^{2L} \left| \sum_{k=0}^{N} h(k) e^{2\pi jkf} \right|^2 df \qquad Eq.3$$

where, $h(k)$, $0 \le k \le N$ are the $(N+1)$ tap FIR filter coefficients. The optimum FIR filter coefficients resulting from the minimization of ψ subject to the condition that the filter has unity dc gain, are given by :

$$h(k) = \frac{{}^{L+k}C_L . {}^{L+N-k}C_L}{{}^{N+2L+1}C_{2L+1}} \approx \frac{30}{N}\left(\frac{k}{N}\right)^2\left(1-\frac{k}{N}\right)^2 \qquad Eq.4$$

where, ${}^nC_k$ = !n / { !k . !(n-k)} and !n denotes the factorial function i.e. !n = 1.2.3........n.

Note that at low frequencies the transfer function of the optimum filter can be approximated as follows :

$$H(f)=\sum_{k=0}^{N} h(k).e^{-j2\pi fk}\approx 1-\frac{15}{112}(\pi fN)^2 \qquad Eq.5$$

The expression in equation 5 can also be used to account for the roll-off of the filter at low frequencies.

3.2 Sinc^k / Comb filters:

An N tap Sinc filter is defined by :

$$h(k)=1/N \quad (0\le k\le N-1) \qquad Eq.6$$

As the filter coefficients resemble a comb in time domain, they are also popularly known as comb filters. An N-tap sinc^K filter is a cascade of K (N/K)-tap filters. Hence the amplitude response of a Sinc^K filter is given by :

$$|H(f)|=\left|K\frac{\sin(\pi fN/K)}{N.\sin(\pi f)}\right|^K\approx 1-\frac{K.(\pi.f)^2}{6}\left(\left(\frac{N}{K}\right)^2-1\right) \qquad Eq.7$$

The approximation on the right hand side of above equation is valid for low frequencies. A linear relationship can be established between the order of the modulator used and the number of Sinc filters in cascade. Usually, a sinc^{L+1} filter is chosen to reduce the quantization noise of a Lth order modulator.

For the optimum FIR filter and the comb filter, the filtered noise power ψ is given by the following equations :

i) Double loop sigma-delta modulation

Optimum FIR filter $\qquad \psi \approx 60 / N^5$

Sinc^3 filter $\qquad \psi \approx 243 / 2 N^5$

ii) Triple loop sigma-delta modulation

Optimum FIR filter $\qquad \psi \approx 8400 / N^7$

Sinc^4 filter $\qquad \psi \approx 81920 / 3 N^7 \qquad Eq.8$

3.3 Comparison of demodulators

As can be seen from equation 8, the optimum FIR filter is associated with a lower noise power. It also has a sharper cutoff and has fewer ripples in the stopband. However, the comb filters have constant coefficients due to which they can be implemented easily by using a recursive loop or using shift registers. Due to this, comb filters are widely preferred.

As noted before both optimum FIR and comb filters show a gradual roll-off of the amplitude response. Although this effect is marginal in most modulator applications, it could be of concern in the multiplier free FIR filter design. If so, to keep unity gain in the passband, a function to compensate the effect of frequency roll-off can be incorporated into the design. This function is obtained by inverting the values of the passband filter transfer functions shown in equations 5 and 7.

3.4 Filtered Quantization Noise Spectral Characteristics:

In this section, the spectrum of the filtered quantization noise is investigated. This is necessary for the multiplier free FIR filter design, which will be discussed in section 4. For the three Σ-Δ modulator architectures, filtered quantization noise is obtained by subtracting the input dc signal from the modulated output. The convolution of the noise and optimum filter taps is decimated and the final power spectral density is obtained using a Hanning window.

The quantization noise spectra of Figure 3 are obtained using optimum FIR filters with *N=128*. The noise power in Figure 3 confirms with the values predicted theoretically by equation 8. (The predicted values are shown in dark lines in Figure 3.) As can be seen all DSM2, MASH3 and LADF3 are meeting the theoretically calculated values. Note that LADF3 modulator gives *20-dB* higher noise power than the MASH3. It can also be seen that while DSM2 and MASH3 provide uniform distribution of filtered noise over the passband, the LADF3 modulator's filtered noise tends to be distributed towards higher frequencies. Note that spectral plots similar to those in Figure 3 could also be obtained for the case of using comb filters in the demodulator.

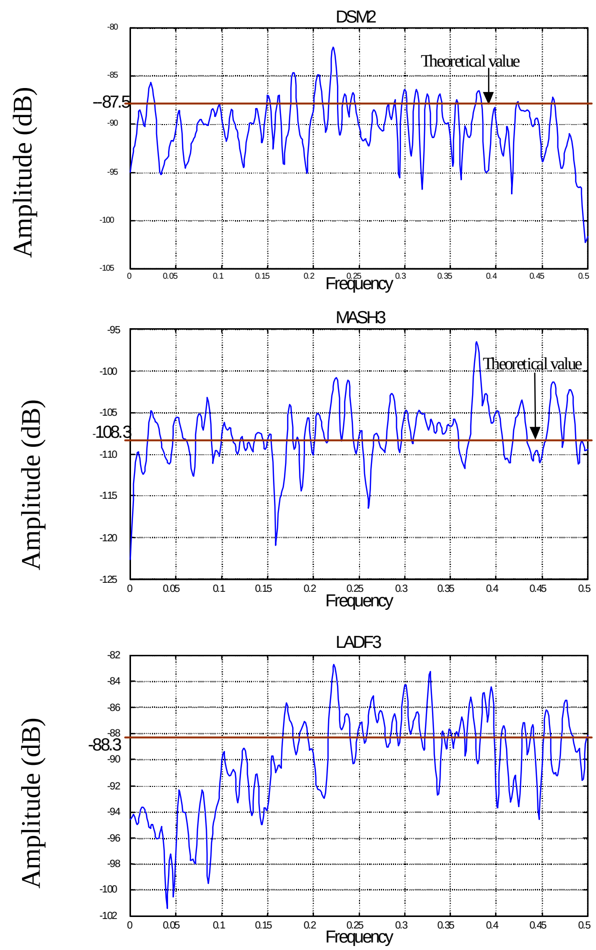

Figure 3: Quantization Noise Spectral Characteristics of Different Modulators Resulting from Optimum FIR Filters

4. DESIGN OF FIR FILTERS USING Σ–Δ MODULATED COEFFICIENTS

This section delves into the design of FIR filters that can be implemented without multipliers using Σ–Δ modulation techniques. The principles are similar to those discussed by Wong and Gray in [9], but here a complete design methodology to meet FIR filter specifications will be provided. Three Σ–Δ based multiplier free FIR filter architectures can be obtained by:

i) Σ–Δ modulating the FIR filter coefficients,

ii) Σ–Δ modulating the input,

iii) Σ–Δ modulating both the input and the filter coefficients.

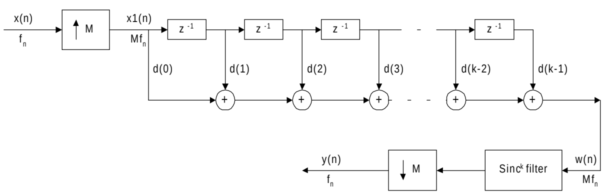

Figure 4: Design of FIR filter with coefficients Σ–Δ modulated.

Here, we discuss architecture (i) in detail. Though architectures (ii) and (iii) have specific advantages of requiring less hardware and can be implemented without adders and multipliers, they can only be used with Σ–Δ modulated inputs, thus limiting their application. On the other hand, architecture (i) can be used with any type of input.

A FIR filter implemented using architecture (i) is shown in Figure 4. The $sinc^k$ filter and the downsampler act as the decoder circuit. They also reduce the quantization noise and prevent aliasing. The important step in designing the circuit in Figure 4 is the selection of oversampling ratio, *M*. The selection of *M*, which depends on the desired FIR filter specifications, will be discussed later in section 4.3. Once *M* is selected, the remaining design steps can be summarized as follows:

(i) Obtain a set of FIR filter coefficients to meet the specifications using any standard filter design technique, e.g. the Remez exchange algorithm.

(ii) Ideally interpolate the FIR filter coefficients by a factor of *M*. Usually an FFT interpolation technique can be used at this step.

(iii) From the ideally interpolated filter coefficients obtain Σ–Δ modulated FIR filter coefficients. These coefficients, denoted *d(n)* in Figure 4, can take the values of {-1, 0, +1}.

(iv) Upsample the input signal (that is required to be processed) by a factor *M* before filtering by *d(n).* Since *d(n)* is +1, 0 or -1, multipliers in Figure 4 can be implemented using an inverter and a switch.

(v) Lowpass filter by a comb filter and decimate by a factor *M* to obtain the filtered output.

Some further design issues of the circuit in Figure 4 are discussed in the following sections.

4.1 Interpolator / Upsampler:

Because of the oversampling architecture, it is necessary to have an interpolator at the input of Figure 4 to increase the sampling rate by a factor *M*. In general, ideal interpolation needs multipliers which is not an option for this design. As an alternative interpolation technique, *(M-1)* zeros can be inserted in between the input samples. However such an interpolation increases the quantization noise power by a factor of *M* when downsampled.

Here a new interpolation method is proposed for the input stage of the circuit in Figure 4. This method is simple but yet effective and does not employ multipliers in the hardware design. The idea here is to copy the input *(M-1)* times in between successive samples. Note that the frequency response of such an interpolation technique is given by :

$$X1(f) = \sum_{n=0}^{MP-1} x1(n)e^{-j2\pi fn} = \frac{1-e^{-j2\pi fM}}{1-e^{-j2\pi f}} X(f) = \frac{Sin\pi fM}{Sin\pi f}\left|X(fM)\right| \qquad Eq.9$$

where, *x1(n)* is the upsampled input and *x(n)* is the input to the architecture. As can be seen, the method contributes an additional *Sinc* factor to the FIR filter frequency response. The additional roll-off in the low frequency components due to the *Sinc* term can be compensated if necessary. This compensation for roll-off can be applied during the interpolated FIR filter coefficient design i.e. in stage (ii) of the previous section.

4.2 Decimation using Comb / $Sinc^k$ filters:

The number of taps of the $sinc^k$ filter, *N*, is usually the same as the upsampling factor *M*. However, a higher value for *N* could also be selected at the cost of increasing the delay of the filter, which is inversely related to the bandwidth. The bandwidth of the filter should be such that the low frequency signal falls within the passband. If *N* is too large the high frequency contents of the signal will be reduced.

4.3 Selection of M:

Let the stopband ripple specified in the original FIR filter requirement be *b*. Suppose we use a LADF3 architecture in the filter design and signal upsampling is obtained by copying *M* signal inputs. Combining equations 2 and 8 we can obtain an expression for the filtered quantization noise level (as shown in Figure 3). Using this expression, to meet the filter stopband ripple requirement, the following inequality can be obtained.

$$\left(\frac{b}{M}\right)^2 \geq \frac{81290*100}{3N^7} \qquad Eq.10$$

The factor of *100* is included in the numerator to compensate for the *20dB* higher noise power level of the LADF3 modulator in comparison to the MASH3 modulator. The factor *M* in equation 10 is due to sample rate increase, i. e. copying the input signal *(M-1)* times. Once the ratio *(N/M)* is decided as discussed in previous section, equation 10 can be used to obtain the value of oversampling ratio, *M*.

5. A DESIGN EXAMPLE

The use of LADF Σ–Δ modulator architecture in the design of a lowpass FIR filter is presented in this section. In the design example, the lowpass filter specifications were selected as follows :

(a) passband frequency edge : 0.10

(b) stopband frequency edge : 0.15

(c) passband ripple : 0.01

(d) stopband ripple : 0.01

Note that all frequencies are normalized quantities. Via the Remez exchange algorithm a FIR filter of length *64* can be easily designed to meet the above specifications. Using stopband ripple (i.e. $b = 0.01$) in equation 10 with $N=M$ results in $M>122$. Selecting $M=128$, and following the steps (i) to (v) of Section 4 it is possible to obtain *8192*, Σ–Δ modulated filter coefficients $d(n)$.

Figure 5(b) shows the transfer functions of the multiplier free FIR filter transfer function obtained from the above procedure for DSM2, LADF3 and MASH3 architecture. (The x-axis shows the normalized frequency.) The transfer function of the original Remez FIR filter is also shown in Figure 5. As can be seen, MASH3 and LADF3 show similar performances and meet the original filter specifications. However, the performance of DSM2 does not meet the specified stopband ripple requirements. For comparison purposes transfer functions resulting from selecting M smaller than the value resulting from equation 10 $(M>122)$ are also shown in Figure 5(a).

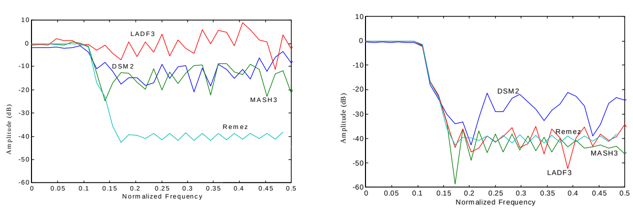

Figure 5: Amplitude Transfer Function of Circuit in Figure 4 .

(a) $M=N=16$; (b) $M=N=128$

Note that in the design of circuit in Figure 4, by using a higher order MASH modulator a lower oversampling rate M would have been achieved. However, this is at the expense of single-bit representation of the output. The major advantage of designing the circuit in Figure 4 using LADF3 architecture is that it can be implemented without using any multipliers. The input signal interpolating technique by copying $(M-1)$ samples, the LADF3 modulated coefficients and the Sinc^k filter all ensure that the hardware can be implemented with adders and shift registers only. Though multipliers have become cheaper over the last decade, multi-bit multipliers are still expensive for VLSI implementations. Besides, the designed architecture can meet higher bit resolution at lower cost, which makes it very lucrative.

6. SUMMARY

Sigma-delta modulators provide high resolution as compared to analogue circuits. Sigma-delta modulation techniques can be effectively used to implement FIR filters. Three Σ–Δ modulator architectures, DSM, LADF and MASH have been compared in this paper in designing multiplier free FIR filters. It has been found that, in general, higher order modulators perform better in terms of noise reduction and lower oversampling ratio requirements. MASH architecture provides lower quantization noise power than LADF architecture. However, because of its architecture, LADF has simplicity in hardware implementation and, therefore, is an appropriate choice for multiplier free FIR filter design.

7. REFERENCES

[1] Stonick J. T., Rulla J. L. and Ardalan S.H., 'Look-ahead decision-feedback sigma-delta modulation', *Proceedings of International conference in Acoustics, speech and signal processing*, 1994, Vol. 3, pp. 541-546.

[2] Veillette, B. R., and Roberts, G. W., 'Delta-Sigma Oscillators: Versatile Building Blocks', *International Journal of Circuit Theory and Applications*, 1997, Vol. 25, pp. 407-418.

[3] Abeysekera S. S., 'Sigma-Delta Architectures for Pulse-Stuffing Synchronizers', *International Journal of Circuit Theory and Applications*, 1997, Vol. 25, pp. 457-467.

[4] Wong P. W., 'Fully Sigma-Delta Modulation encoded FIR filters', *IEEE Transactions on Signal Processing*, 1992, Vol. 40, No. 6, pp. 1605-1609.

[5] Ning He, Frederico Kuhlmann and Andres Buzo, 'Double-loop sigma-delta modulation with dc input', *IEEE transactions on Communications*, 1990, Vol. 38, No. 4, pp. 487 – 495.

[6] Uchimura K., Hayashi T., Kimura and Iwata A., 'Oversampling A-to-D and D-to-A converters with multistage noise shaping modulators', *IEEE Transactions on Acoustics, Speech and Signal Processing*, 1988, Vol. 36, No. 12, pp. 1899-1905.

[7] Matsuya Y., Uchimura K., Kobayashi T., Kimura, Ishikawa M., Yoshitome T. and Iwata A., 'A 16-bit oversampling A-to-D conversion technology using triple-integration noise shaping', *IEEE Journal of solid-state circuits*, 1987, Vol. 22, No. 6, pp. 921-928.

[8] Wu C., Wong P. W. and Gray R. M., 'Multistage Sigma-Delta modulation', *IEEE Transactions on Information theory*, 1989, Vol. 35, pp. 784 - 796.

[9] Wong, P. W. and Gray, R. M.,'FIR filters with Sigma-Delta modulation encoding', *IEEE Transactions on Acoustics, Speech and Signal Processing*, 1990, Vol. 38, No. 6, pp. 979 - 989.

[10] Abeysekera S. S., Xue Yao, and Zang Z., 'Comparison of Various Lowpass Filter Architectures for Sigma-Delta Demodulators', *International Symposium on Circuits and Systems - ISCAS '99*, (to appear) Orlando, Florida, U.S.A., June 1999.